Interaction between coaxial dielectric disks enhances the Q factor

Cite as: J. Appl. Phys. **126**, 093105 (2019); https://doi.org/10.1063/1.5094188
Submitted: 27 February 2019 . Accepted: 21 July 2019 . Published Online: 06 September 2019

K. N. Pichugin, and A. F. Sadreev

Journal of Applied Physics ARTICLE scitation.org/journal/jap

Interaction between coaxial dielectric disks enhances the Q factor

Cite as: J. Appl. Phys. **126**, 093105 (2019); doi: 10.1063/1.5094188
Submitted: 27 February 2019 · Accepted: 21 July 2019 ·
Published Online: 6 September 2019

K. N. Pichugin[1,2] and A. F. Sadreev[1,a)]

AFFILIATIONS

[1]Kirensky Institute of Physics, Federal Research Center KSC SB RAS, 660036 Krasnoyarsk, Russia
[2]Reshetnev Siberian State University of Science and Technology, 660037 Krasnoyarsk, Russia

Note: This paper is part of the Special Topic on Dielectric Nanoresonators and Metamaterials.
[a)]**Electronic mail:** almas@tnp.krasn.ru

ABSTRACT

We study the behavior of resonant modes under variation of the distance between two coaxial dielectric disks and show an avoided crossing of resonances because of the interaction between the disks. Owing to coaxial arrangement of disks, the resonant modes are specified by the azimuthal index $m = 0, 1, 2, \ldots$. In the present paper, we consider the case $m = 0$. At a long enough distance, the modes are symmetric and antisymmetric hybridizations of the resonant modes of the isolated disk. With decreasing the distance, the interaction becomes stronger, giving rise to avoided crossings of different resonances of the isolated disk. This in turn enhances the Q factor of the two disks by one order in magnitude compared to the Q factor of the isolated disk.

I. INTRODUCTION

Optical microcavities and various other sorts of resonators have been widely employed to tightly localize electromagnetic field in small volumes for a long duration due to high Q factors, which plays an indispensable role in lasing, sensing, filtering, and many other applications in both the linear and nonlinear regimes. In general, there is a compromise between high Q factors and small mode volumes due to the fact that larger resonators are required to increase the round-trip travel time for Q factor enhancement, as is the case for whispering gallery modes.[1,2]

It is rather challenging for optical resonators to support resonances of simultaneous subwavelength mode volumes and high Q factors. The traditional way for increasing the Q factor of optical cavities is suppression of leakage of a resonance mode into the radiation continua. This is usually achieved by decreasing the coupling of the resonant mode with the continua. However, microcavities and resonators based on reflection from their boundaries demonstrate low values of the Q factor by virtue of weakness of the dielectric contrast of optical materials. The conventional ways to realize high Q resonators are the use of metals, photonic bandgap structures, or whispering gallery mode resonators. All of these approaches lead to reduced device efficiencies because of complex designs, inevitable metallic losses, or large cavity sizes. On the contrary, all-dielectric subwavelength nanoparticles have recently been suggested as an important pathway to enhance capabilities of traditional nanoscale resonators by exploiting the multipolar Mie resonances being limited only by radiation losses.[3,4]

The decisive breakthrough came from the paper by Friedrich and Wintgen,[5] which put forward the idea of destructive interference of two neighboring resonant modes leaking into the continuum. Based on a simple generic two-level model, they formulated the condition for a bound state in the continuum (BIC) as the state with zero resonant width at crossing of two eigenfrequencies of the cavity. This principle was later explored in an open plane wave resonator where the BIC occurs with degeneracy of resonant frequencies.[6]

However, these BICs exist provided that they embedded into a single continuum of propagating modes of a directional waveguide. In photonics, the optical BICs embedded into the radiation continuum can be realized in two ways. The first way is the use of an optical cavity coupled with the continuum of a 2D photonic crystal (PhC) waveguide[7] that is an optical analog of the microwave system.[6] A more perspective way is to achieve BICs in periodic PhC systems or arrays of dielectric particles in which resonant modes leak into a restricted number of diffraction continua.[8–12] Although the exact BICs can exist only in infinite periodical arrays,[13,14] the finite arrays

demonstrate resonant modes with a very high Q factor, which grows quadratically with the number of particles[15] (quasi-BICs).

Another attractive way to achieve quasi-BICs (supercavity modes) is to use individual subwavelength high-index dielectric resonators, which also exhibit high Q factors.[4,16–18] Such super cavity modes originate from avoided crossing of the resonant modes, specifically the Mie-type resonant mode and the Fabry–Pérot resonant mode under variation of the aspect ratio of the dielectric disk. As a result, a significant enhancement of the Q factor is reported. It is worth noticing that the idea of formation of long-lived, scarlike modes near avoided crossings in optical deformed microcavities was first put forward by Wiersig.[19] The dramatic Q factor enhancement was predicted by Boriskina[20,21] at an avoided crossing of highly excited whispering gallery modes in symmetrical photonic molecules of dielectric cylinders.

In the present paper, we consider a similar way to enhance the Q factor by variation of the distance between two identical coaxial dielectric disks. In contrast to Refs. 19–23, we consider the avoided crossing of low excited resonant modes (monopole and dipole). When the disks are separated by a long distance, we have pairs of almost degenerate resonant modes. With the decrease of the distance, the resonant modes interfere giving rise to avoided crossings. We show that this effect is complemented with a spiral behavior of the resonant eigenfrequencies when the interaction between the disks is weak. With a further decrease of the distance, the interaction is increasing to give rise to a strong repulsion of the resonances. In this phenomenon, one of the resonant eigenfrequencies can closely approach to the real axis acquiring the Q factor much higher than that of the isolated disk.

II. AVOIDED CROSSING IN THE SYSTEM OF TWO COAXIAL DISKS

There are two limiting cases of the system of coaxial dielectric disks, the infinite periodic array of disks and the isolated disk. The former supports numerous BICs: symmetry protected BICs in the Γ-point, accidental BICs with a nonzero Bloch vector, and hybrid BICs with nonzero orbital angular momentum.[24] The symmetry protected BICs were experimentally observed in the system of ceramic disks in the THz range.[15] The case of the isolated disk was considered in papers,[4,16] which have shown considerable enhancement of the Q factor due to an avoided crossing of two resonant modes. In these papers, the avoided crossing was achieved through variation of the aspect ratio of the disk, which technologically is not simple. In the present section, we consider two identical coaxial disks as sketched in Fig. 1 with the aspect ratio not obligatory tuned to the optimal Q factor as in Refs. 16 and 18. The coaxial disks have the advantage that all resonant modes are classified by the azimuthal number $m = 0, 1, 2, \ldots$ because of the axial symmetry. Therefore, one can consider subspaces with definite m separately. In the present paper, we consider the case $m = 0$ in which the solutions are separated by polarization with $H_z = 0$ (E modes) and $E_z = 0$ (H modes). In what follows, we consider the H-modes.

In general, the resonant modes and their eigenfrequencies are found by solving the time-harmonic source-free Maxwell

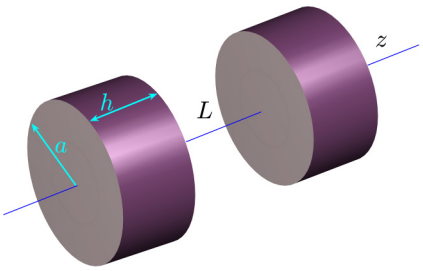

FIG. 1. Two coaxial dielectric disks separated by distance L measured between the centers of disks.

equations,[25,26]

$$\begin{pmatrix} 0 & \frac{i}{\epsilon}\nabla\times \\ -i\nabla\times & 0 \end{pmatrix}\begin{pmatrix} \mathbf{E}_n \\ \mathbf{H}_n \end{pmatrix} = k_n \begin{pmatrix} \mathbf{E}_n \\ \mathbf{H}_n \end{pmatrix}, \tag{1}$$

where $\mathbf{E}_n$ and $\mathbf{H}_n$ are the EM field components defined in Ref. 26 as quasinormal modes, which are also known as resonant states[27,28] or leaky modes.[29] It is important that they can be normalized and the orthogonality relation can be fulfilled by the use of perfectly matched layers (PMLs).[26] With the exception of symmetrical particles, cylinders, spheres, etc., Eq. (1) can be solved only numerically, in particular, by COMSOL Multiphysics. Irrespective of the choice of the dielectric particle, the eigenfrequencies are complex, $k_n a = \omega_n + i\gamma_n$, where a is the disk radius. In what follows, the light velocity is taken as a unit. Figure 2 shows resonant frequencies of the isolated disk complemented with their mode profiles (only E_ϕ is shown). There are modes with nodal surfaces crossing the z axis and the modes with nodal surfaces crossing the plane $z = 0$. They are the Fabry–Perót resonant modes and the radial Mie modes introduced in Ref. 16, correspondingly.

Figure 3 shows the solutions of Eq. (1) for two coaxial dielectric disks with variation of the distance L between the disks. The

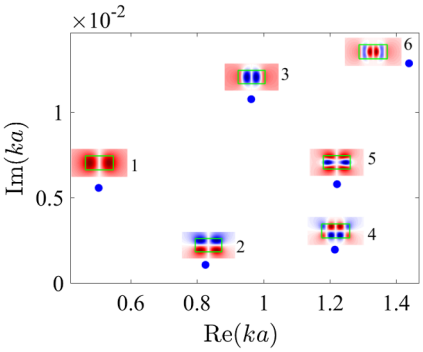

FIG. 2. The resonant eigenfrequencies (closed circles) and the corresponding resonant modes (the component E_ϕ) of the dielectric disk with the height $h = a$ and permittivity $\epsilon = 40$.

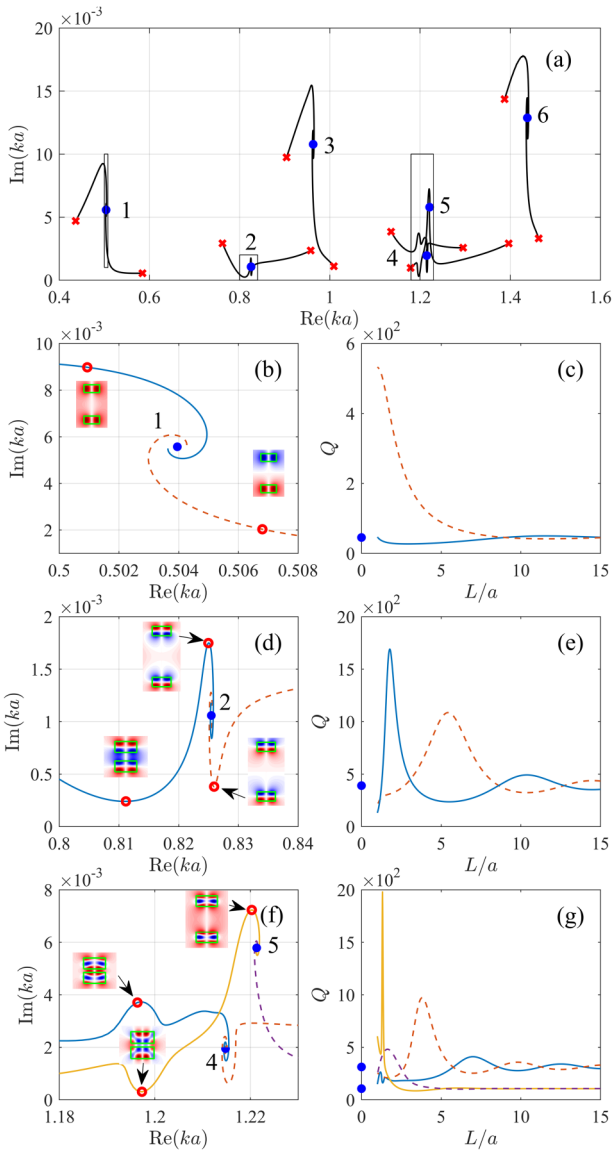

FIG. 3. (a) Behavior of resonant eigenfrequencies under variation of the distance between the disks L with the same parameters as in Fig. 2. (b), (d), and (f) Zoomed areas highlighted in (a) with symmetric (solid lines) and antisymmetric (dash lines) hybridization (6) of resonant modes of the isolated disk. (c), (e), and (g) show behavior of the Q factor vs the distance for corresponding insets at the left. Closed blue circles mark the eigenfrequencies of isolated disks and, respectively, the Q factors, while crosses mark the limiting case $L = h$ when two disks stick together.

necessity to use PMLs restricts the distance between the disks, which is to be considerably less than the distance between the PMLs in the z-direction. In spite of an illusive complexity in Fig. 3(a), the zoomed pictures reveal remarkably simple behavior of resonant frequencies in the form of a spiral convergence of avoided eigenfrequencies to the resonant frequencies of the isolated disks marked by closed circles as demonstrated in Figs. 3(b), 3(d), and 3(f) in zoomed plots. However, when the disks are close enough to each other, the spiraling behavior is replaced by a strong repulsion of the complex eigenfrequencies because of stronger coupling between the disks.Figures 3(e) and 3(g) show the oscillating behavior of the Q factors, while Fig. 3(c) demonstrates a rapid decline of the Q factor with the distance between disks. The Q factor was calculated as the ratio of real part and imaginary parts of the resonant eigenfrequency: $Q = \mathrm{Re}(ka)/2\mathrm{Im}(ka)$. The aforementioned difference in dependencies of the Q factor vs the distance between the disks is directly related to the radiation patterns of resonant modes shown in Fig. 2. The radiation from one disk scatters from the other resulting in a coupling between the disks. The general expression for the coupling between dielectric resonators was considered in Refs. 30–32,

$$\kappa = \int d^3\vec{x}[\epsilon(\vec{r}) - 1]\vec{E}_1^{*}\vec{E}_2, \tag{2}$$

where $\vec{E}_{1,2}$ are the PML-normalized solutions for the separated disks.[26] One can see that the coupling is determined by overlapping of the resonant modes, which in turn depends on the distance between the particles. Moreover, the overlapping also depends on the number of wavelengths stacked over the z axis in the radiation modes shown in Fig. 2.

In order to quantitatively evaluate this interaction, we consider an isolated disk for which the matrix of derivatives in Eq. (1) becomes diagonal with the complex eigenfrequencies k_n in the eigenbasis presented in Fig. 2. It is reasonable to consider that for a large distance between the disks, the matrix is still diagonal with pairs of degenerate k_n shown in Fig. 3 by blue closed circles. Rigorously speaking for the large distance between the disks $L \gg a/\gamma_n$, the interaction via the resonant modes can grow exponentially.[26] In view of that, we restrict the distance $L < a/\gamma_n$. As the distance between the disks is reduced, the interaction between the disks via the resonant modes splits the degenerate eigenfrequencies k_n giving rise to the avoided crossing. Assume also that the value of splitting is much less than the distance between the different k_n. These assumptions are justified numerically as shown in the insets to Fig. 3, however, only for certain domains of the eigenfrequency k around the resonances of the isolated disk where the spiral behavior takes place. In the framework of these assumptions, we can use a two-mode approximation for the Hamiltonian matrix in Eq. (1) for each resonance k_n,[18,19,26]

$$H_{eff}^{(n)} = H_{eff}^{(0)} + V = \begin{pmatrix} k_n a & 0 \\ 0 & k_n a \end{pmatrix} + \begin{pmatrix} u_n & v_n \\ v_n & u_n \end{pmatrix}, \tag{3}$$

where v_n is responsible for the interaction between the disks via the resonant modes, while u_n is the result of the backscattering. Therefore, one can expect that $\arg(v_n) = \omega_n L/a$, $\arg(u_n) = 2\omega_n L/a$. Figure 4 shows the behavior of both the absolute value and phase of the matrix elements. The matrix elements v_n and u_n can be easily found from numerically calculated resonances shown in

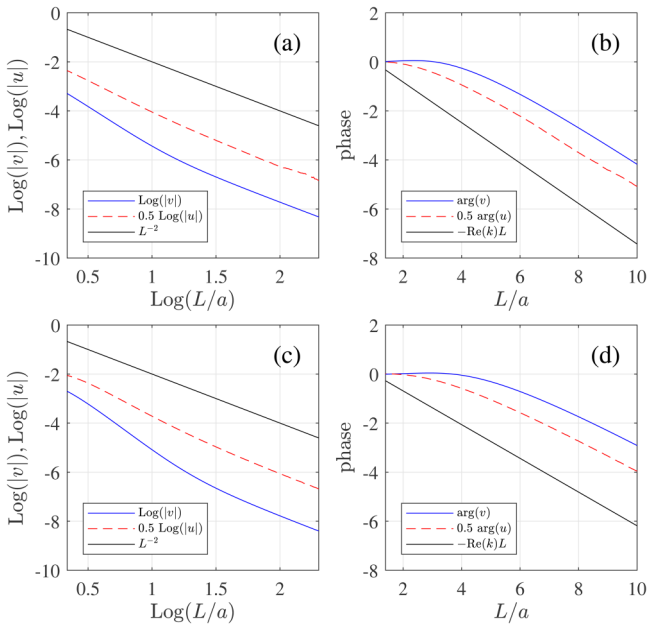

FIG. 4. Dependence of the matrix elements v_n and u_n on the distance between disks L. (a) and (b) were evaluated according to Fig. 3(b), while (c) and (d) were evaluated according to Fig. 6(b).

Figs. 3(b) and 3(d),

$$k_{a,s}^{(n)} a = k_n a + u_n \pm v_n, \tag{4}$$

as $v_n = \frac{k_s^{(n)} - k_a^{(n)}}{2}$, $u_n = \frac{k_s^{(n)} + k_a^{(n)}}{2} - k_n$. As a result, we obtain (3)

$$v_n \sim \frac{e^{-ik_n L}}{L^2}, \quad u_n \sim \frac{e^{-2ik_n L}}{L^4}. \tag{5}$$

The scaling law against the distance (5) is observed with good accuracy for all resonances shown in Fig. 3, however, for only

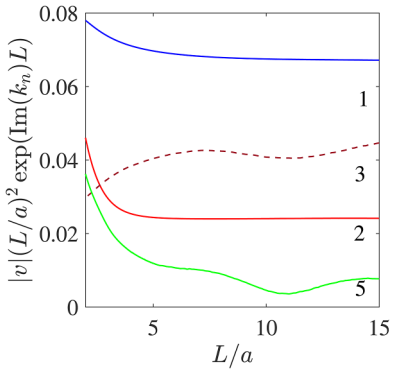

FIG. 5. Dependence of the coupling $|v_n|$ on the distance between disks L.

regimes of spiral convergence of the resonances. The numerically calculated behavior of the matrix elements v_n and u_n for $n = 2$ is shown in Fig. 4. In spiralling around the resonances of the isolated disk, the hybridized resonant eigenmode is given by symmetric and antisymmetric combinations of the resonant modes of the isolated disk,

$$\psi_{s,a}(\vec{r}) \approx \psi_n\left(\vec{r}_\perp - \frac{1}{2}L\vec{z}\right) \pm \psi_n\left(\vec{r}_\perp + \frac{1}{2}L\vec{z}\right), \tag{6}$$

where $\vec{r}_\perp = r, \phi$, $\vec{z}$ is the unit vector along the z axis and $\psi_n(\vec{r}_\perp)$ is the corresponding resonant mode of the isolated disk shown in the insets of Fig. 2.

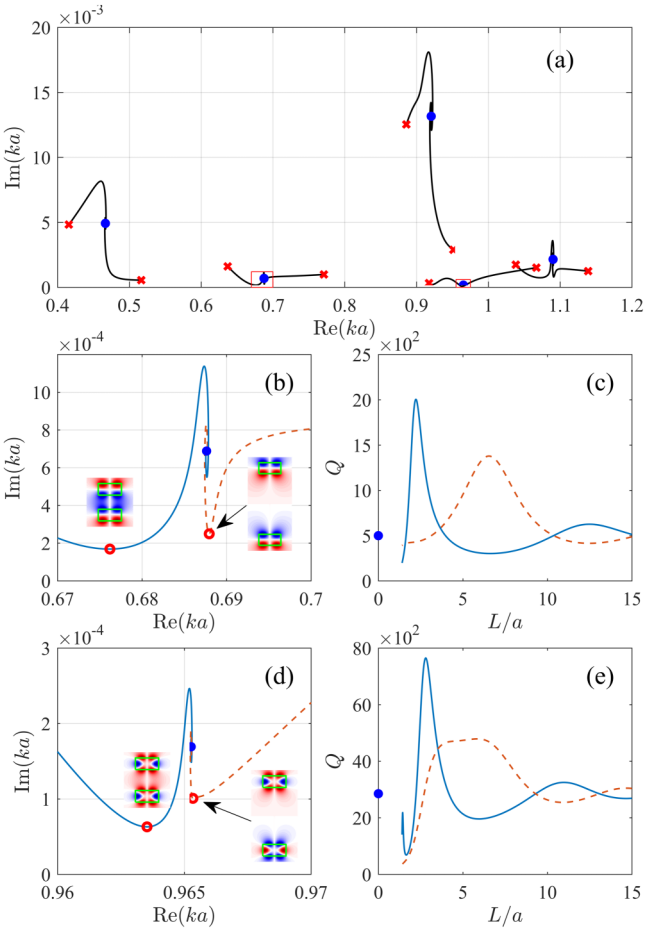

FIG. 6. (a) Behavior of resonant eigenfrequencies under variation of the distance between the disks L with $\epsilon = 40$ (ceramics in the terahertz range) and the aspect ratio $a/h = 0.7$. (b) and (d) Zoomed areas highlighted in (a) with symmetric (solid lines) and antisymmetric (dashed lines) hybridization (6) of resonant modes of the isolated disk. (c) and (e) show behavior of the Q factor vs the distance for corresponding insets at the left. Closed circles mark the eigenfrequencies of isolated disks and, respectively, the Q factors, while crosses mark the limiting case $L = 1$ when two disks stick together.

In Fig. 5, we show the dependence of the coupling constant ν_n on the distance calculated in the two-level approximation. One can see that the higher the Fabry–Perót resonance with indices 1 or 3, 2 or 4, 5 according to Fig. 2, the weaker the coupling shown in Fig. 5, and, respectively, the more spiral evolution of resonances as indeed Figs. 3(b), 3(d), and 3(f) evident. In order to better distinguish the true couplings between the disks, we absorb the contribution e^{-ik_nL}/L^2 onto the ν_n in accordance with Eq. (5). Figure 5 shows that these couplings through mode 1 are so large that the resonances $k_{a,s}^{(1)}$ quickly avoid each other, while for other resonances $k_{a,s}^{(n)}$, $n > 1$, the coupling is sufficiently weak to show an avoided crossing in the form of spiral evolution. Respectively, we observe different dependencies of the Q factors presented in Figs. 3(c), 3(e), and 3(g).

At first, the resonant frequencies go away from the limiting point given by k_n. Respectively, the Q factor in Fig. 3(c) demonstrates oscillating behavior exceeding the Q factor of the isolated disk several times. As the disks approach one another, the spiral behavior of the pair of resonances $k_{s,a}^{(n)}$ is replaced by strong repulsion as shown in Fig. 3(a). Figure 3(d) shows a remarkable feature caused by the avoided crossing of resonances with different n. To be specific, there is an avoided crossing of symmetric resonances $k_s^{(2)}$ and $k_s^{(5)}$ according to notations in Fig. 2. Because of the same symmetry of the resonances relative to $z \to -z$, they undergo the typical avoided crossing with a considerable decrease of the imaginary part of the resonant frequency and enhancement of the Q factor by one order in magnitude. Respectively, the two-mode approximation (3) breaks down.

It is interesting to trace the behavior of the resonances and Q factors for the aspect ratio $a/h \approx 0.7$ and $\epsilon = 40$ for which the isolated disk shows the maximal Q factor.[4,16] The results are presented in Fig. 6. One can see that with decrease of the distance between the disks, we have the same spiralling behavior of the hybridized resonances around the resonances of the isolated disks, which is terminated by strong repulsion of the symmetric and antisymmetric resonances for $L \to h$. However, we have no pronounced effect of the avoided crossing of hybridized resonances with different n and, respectively, have no enhancement of the Q factor by one order as it was achieved for the aspect ratio $a/h = 1$ [see Fig. 6(e)].

Until now, we considered the permittivity $\epsilon = 40$ and $a = 1$ cm (ceramic disks) that corresponds to the resonant frequencies into the terahertz range. Finally, we consider $\epsilon = 12$ (silicon disks) and $a = h = 1\mu$ with the resonant frequencies in the optical range. The results of computations are presented in Fig. 7, which shows that there is no qualitative difference between the ceramic disks and silicon disks. Similar to Figs. 3 and 6, we observe spiral behavior of the resonant eigenfrequencies for enough distance between the disks. However, what is more remarkable that we also observe the avoided crossing of the resonances with different n as shown in Fig. 7(d) with corresponding strong enhancement of the Q factor by one order in magnitude [Fig. 7(e)].

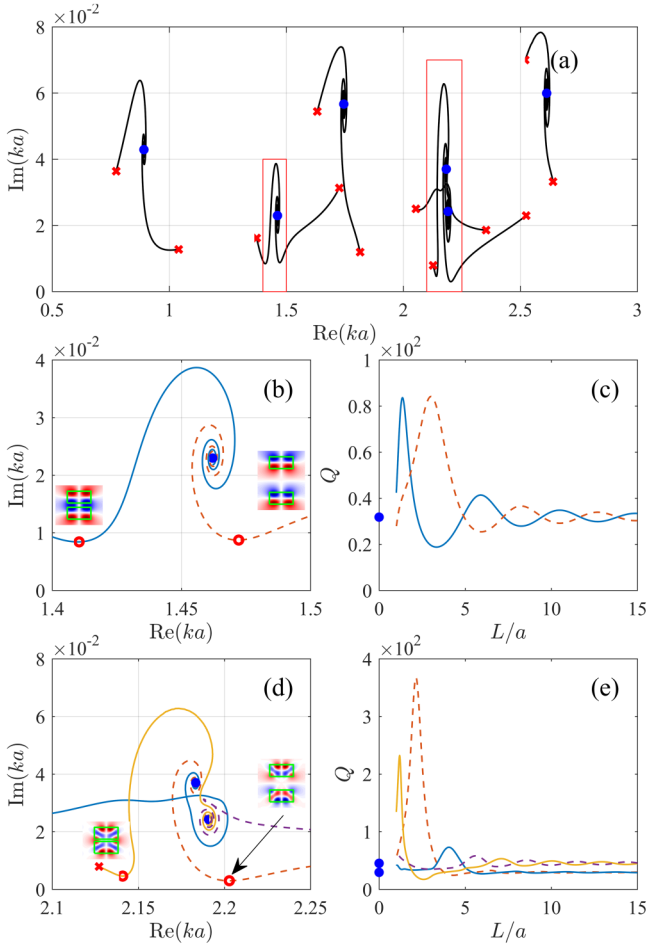

FIG. 7. (a) Behavior of resonant eigenfrequencies under variation of the distance between the disks L with $\epsilon = 12$ (silica in the optical range) and the aspect ratio $a/h = 1$. (b) and (d) Zoomed areas highlighted in (a) with symmetric (solid lines) and antisymmetric (dashed lines) hybridization (6) of resonant modes of the isolated disk. (c) and (e) show behavior of the Q factor vs the distance for corresponding insets at the left. Closed circles mark the eigenfrequencies of isolated disks and, respectively, the Q factors, while crosses mark the limiting case $L = 1$ when two disks stick together.

III. CONCLUSIONS

The recipe to enhance the Q factor by means of the avoided crossing of resonances is well known. Friedrich and Wintgen[5] were the first who investigated the quantitative influence of the interference of resonances on their positions and widths. Moreover, in the framework of two-level effective Hamiltonian, they found out that one of the widths can turn to zero to identify a BIC. A single isolated dielectric particle of finite dimensions cannot trap light[13] because of the infinite number of radiation continua or diffraction channels.[12] However, with a sufficiently large refractive index, the particle shows distinctive Mie resonances with the Q factors, which can be substantially enhanced owing to the avoided crossing of the resonances under variation of the aspect ratio.[18,33] Technologically, it might be challenging to vary the size of the disk in the optical range. In the present paper, we propose to vary the distance between two coaxial disks that is preferable from the experimental

viewpoint. Continuous variation of the distance gives rise to an avoided crossing of the Mie resonances due to the interaction between the disks through radiating resonant modes.

If there is enough distance, we can assume that two disks have almost degenerate resonances k_n. However, as the distance is decreased, the disks weakly couple with each other via the leaky resonant modes. This lifts a degeneracy of the resonances according to Eq. (4) and results in symmetric and antisymmetric hybridizations of resonant modes $k_{s,a}^{(n)}$ according to Eq. (6). As a result, we observe a spiral avoided crossing of the resonances around the points k_n. A further decrease of the distance between the disks enhances the interaction and, respectively, gives rise to strong repulsion of $k_s^{(n)}$ and $k_a^{(n)}$. However, what is most remarkable is that there are avoided crossings of the resonances with different n. Respectively, one can observe strong enhancement of the Q factor around one order in magnitude.

Although in the present paper we only considered dielectric disks, it is clear that the phenomenon of the avoided crossing and respective enhancement of the Q factor would occur with particles of arbitrary shape when the distance between them is varied. The case of two coaxial disks simplifies computations because the solutions with different angular momentum m are independent. In the present paper, we have presented only the case $m = 0$ because of a possibility to consider E-modes and H-modes separately.

ACKNOWLEDGMENTS

We are grateful to A. A. Bogdanov, E. N. Bulgakov, and D. N. Maksimov for numerous and fruitful discussions. This work was supported by the Russian Federation for Basic Research (RFBR) (Grant No. 19-02-00055) and Ministry of Education and Science of Russian Federation (State Contract No. 3.1845.2017).

REFERENCES

[1]V. Braginsky, M. Gorodetsky, and V. Ilchenko, "Quality-factor and nonlinear properties of optical whispering-gallery modes," Phys. Lett. A **137**, 393 (1989).
[2]H. Cao and J. Wiersig, "Dielectric microcavities: Model systems for wave chaos and non-Hermitian physics," Rev. Mod. Phys. **87**, 61 (2015).
[3]A. Kuznetsov, A. Miroshnichenko, M. Brongersma, Y. Kivshar, and B. Luk'yanchuk, "Optically resonant dielectric nanostructures," Science **354**, 2472 (2016).
[4]K. Koshelev, A. Bogdanov, and Y. Kivshar, "Meta-optics and bound states in the continuum," Sci. Bull. **17**, 065601 (2018).
[5]H. Friedrich and D. Wintgen, "Interfering resonances and bound states in the continuum," Phys. Rev. A **32**, 3231 (1985).
[6]A. Sadreev, E. Bulgakov, and I. Rotter, "Bound states in the continuum in open quantum billiards with a variable shape," Phys. Rev. B **73**, 235342 (2006).
[7]E. Bulgakov and A. Sadreev, "Bound states in the continuum in photonic waveguides inspired by defects," Phys. Rev. B **78**, 075105 (2008).
[8]S. P. Shipman and S. Venakides, "Resonant transmission near nonrobust periodic slab modes," Phys. Rev. E **71**, 026611 (2005).
[9]D. C. Marinica, A. G. Borisov, and S. V. Shabanov, "Bound states in the continuum in photonics," Phys. Rev. Lett. **100**, 183902 (2008).
[10]C. W. Hsu, B. Zhen, J. Lee, S. G. Johnson, J. D. Joannopoulos, and M. Soljačić, "Observation of trapped light within the radiation continuum," Nature **499**, 188 (2013).
[11]E. N. Bulgakov and A. F. Sadreev, "Bloch bound states in the radiation continuum in a periodic array of dielectric rods," Phys. Rev. A **90**, 053801 (2014).
[12]E. Bulgakov and A. F. Sadreev, "Bound states in the continuum with high orbital angular momentum in a dielectric rod with periodically modulated permittivity," Phys. Rev. A **96**, 013841 (2017).
[13]D. Colton and R. Kress, *Inverse Acoustic and Electromagnetic Scattering Theory*, 2nd ed. (Springer, Berlin, 1998).
[14]M. G. Silveirinha, "Trapping light in open plasmonic nanostructures," Phys. Rev. A **89**, 023813 (2014).
[15]Z. F. Sadrieva, M. A. Belyakov, M. A. Balezin, P. V. Kapitanova, E. A. Nenasheva, A. F. Sadreev, and A. A. Bogdanov, "Experimental observation of a symmetry-protected bound state in the continuum in a chain of dielectric disks," Phys. Rev. A **99**2019).
[16]M. V. Rybin, K. L. Koshelev, Z. F. Sadrieva, K. B. Samusev, A. A. Bogdanov, M. F. Limonov, and Y. S. Kivshar, "High-Q supercavity modes in subwavelength dielectric resonators," Phys. Rev. Lett. **119**, 243901 (2017).
[17]W. Chen, Y. Chen, and W. Liu, "Multipolar conversion induced subwavelength high-Q supermodes with unidirectional radiations," preprint arXiv:1808.05539 (2018).
[18]A. Bogdanov, K. Koshelev, P. Kapitanova, M. Rybin, S. Gladyshev, Z. Sadrieva, K. Samusev, Y. Kivshar, and M. F. Limonov, "Bound states in the continuum and Fano resonances in the strong mode coupling regime," Adv. Photonics **1**, 1 (2019).
[19]J. Wiersig, "Formation of long-lived, scarlike modes near avoided resonance crossings in optical microcavities," Phys. Rev. Lett. **97**, 253901 (2006).
[20]S. V. Boriskina, "Theoretical prediction of a dramatic q-factor enhancement and degeneracy removal of whispering gallery modes in symmetrical photonic molecules," Opt. Lett. **31**, 338 (2006).
[21]S. Boriskina, "Coupling of whispering-gallery modes in size-mismatched microdisk photonic molecules," Opt. Lett. **32**, 1557 (2007).
[22]J. Unterhinninghofen, J. Wiersig, and M. Hentschel, "Goos-Hanchen shift and localization of optical modes in deformed microcavities," Phys. Rev. E **78**, 016201 (2008).
[23]M. Benyoucef, J.-B. Shim, J. Wiersig, and O. G. Schmidt, "Quality-factor enhancement of supermodes in coupled microdisks," Opt. Lett. **36**, 1317 (2011).
[24]E. N. Bulgakov and A. F. Sadreev, "Bound states in the continuum with high orbital angular momentum in a dielectric rod with periodically modulated permittivity," Phys. Rev. A **96**, 013841 (2017).
[25]R. D. Meade, J. N. Winn, and J. D. Joannopoulos, *Photonic Crystals: Molding the Flow of Light* (Princeton University Press, Princeton, NJ, 1995).
[26]P. Lalanne, W. Yan, K. Vynck, C. Sauvan, and J.-P. Hugonin, "Light interaction with photonic and plasmonic resonances," Laser Photonics Rev. **12**, 1700113 (2018).
[27]R. M. More and E. Gerjuoy, "Properties of resonance wave functions," Phys. Rev. A **7**, 1288 (1973).
[28]E. A. Muljarov, W. Langbein, and R. Zimmermann, "Brillouin-Wigner perturbation theory in open electromagnetic systems," Europhys. Lett. **92**, 50010 (2010).
[29]A. W. Snyder and J. D. Love, *Optical Waveguide Theory* (Springer US, 1984).
[30]I. Awai and Y. Zhang, "Coupling coefficient of resonators—An intuitive way of its understanding," Electron. Commun. Jpn. **90**, 11–18 (2007).
[31]S. Y. Elnaggar, R. J. Tervo, and S. M. Mattar, "General expressions and physical origin of the coupling coefficient of arbitrary tuned coupled electromagnetic resonators," J. Appl. Phys. **118**, 194901 (2015).
[32]A. Tayebi and S. Rice, "Superradiant and dark states in non-Hermitian plasmonic antennas and waveguides," preprint arXiv:1812.10057 (2018).
[33]M. Rybin and Y. Kivshar, "Optical physics: Supercavity lasing," Nature **541**, 164 (2017).